A Differential Fluorescent Receptor for Nucleic Acid Analysis

Hillary N. Bengtson, Dmitry M. Kolpashchikov

Supporting materials

Content

1. **Table S1.** Sequences and concentrations of oligonucleotides used in this study.

DMB1[a]	[20-40 nM] FAM-5'- *CC GAG* TCA AGT TAC TAA C*CT CGG GCT GC* C TAG ATA TGA ACA T*GC AGC*- BH1			
	Adaptor A	*Adaptor B*	*Adaptor C*	*Adaptor D*
Sensor 1	A1: [1200 nM] CGC TTG TGG GTA ACT TG	B1: [800 nM] AGG TTA GTC AAC CCC GAG CCC G	C1: [800 nM] AGG CAC AGC GGG TTG TAT CT	D1: [800 nM] CAT GTT CAT TCT GGT ACA TG
Sensor 2	A2: [1200 nM] CCG ACA GTC G GTA ACT TG	B2: [400 nM] AGG TTA GCG CTT GTG GGG CCC G	C2: [400 nM] AGG CAT CAA CCC CGA TAT CT	D2: [1200 nM] CAT GTT CAC AGC TGG TTG
Sensor 3	A3: [400 nM] TCA ACT CCG AGT AAC TTG	B3: [400 nM] AGG TTA CAG CGG GTT GTG CCC G	C3: [800 nM] AGG CAT CTG GTC CAT TAT CT	D3: [400 nM] CAT GTT CAG AAT TGT TT
Analytes [100 nM]				
WT	5' GC ACC CAG CTG AGC CAA TTC ATG GAC CAG AAC AAC CCG CTG TCG GGG TTG ACC CAC AAG CGC CGA CTG TCG GCG CTG			
MT1[b]	5' GC ACC CAG CTG AGC CAA TTC ATG GAC CAG AAC AAC CCG CTG TCG GGG TTG ACC CAC AAG CGC CGA CTG TGG GCG CTG			
MT2	5' GC ACC CAG CTG AGC CAA TTC ATG GAC CAG AAC AAC CCG CTG TCG GGG TTG ACC CTC AAG CGC CGA CTG TCG GCG CTG			
MT3	5' GC ACC CAG CTG AGC CAA TTC ATG GAC CAG AAC AAC CCG CTG TGG GGG TTG ACC CAC AAG CGC CGA CTG TCG GCG CTG			
MT4	5' GC ACC CAG CTG AGC CAA TTC ATG GAC CAG AAC AAC CCG CTG TTG GGG TTG ACC CAC AAG CGC CGA CTG TCG GCG CTG			
MT5	5' GC ACC CAG CTG AGC CAA TTC ATG GGC CAG AAC AAC CCG CTG TCG GGG TTG ACC CAC AAG CGC CGA CTG TCG GCG CTG			
MT6	5' GC ACC CAG CTG AGC CAA TTC ATG TAC CAG AAC AAC CCG CTG TCG GGG TTG ACC CAC AAG CGC CGA CTG TCG GCG CTG			
MT7	5' GC ACC CAG CTG AGC CCA TTC ATG GAC CAG AAC AAC CCG CTG TCG GGG TTG ACC CAC AAG CGC CGA CTG TCG GCG CTG			

[a]Stem-forming nucleotides of the DMB probe are shown in italics.
[b]Nucleotide substitutions in the sequences of MT1-MT5 are red undelined.

** Adaptor strand concentrations were chosen individually for each sensor based on optimization experiments. Optimization included variation of the concentration of DMB1 and the adaptor strands for each individual TX sensor (data not shown). The main optimization criterion was achieving greatest differentiating, i.e. different signal intensities for the 8 analytes used in this study. Mismatches were introduced into some adaptor strands to reduce stability of their complexes with analyte and, therefore, increase differentiation capability of the sensors.

2. Secondary structures of analytes WT, MT1-MT7.

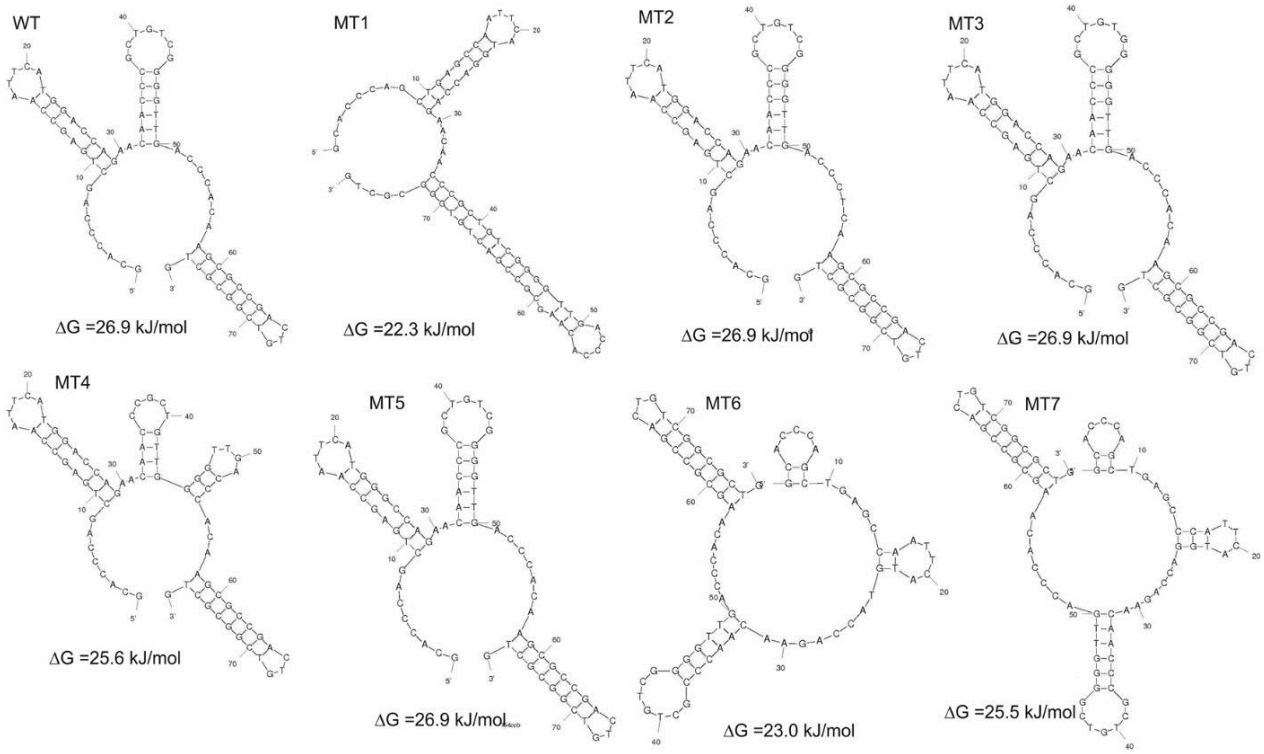

Figure S1. Secondary structures of DNA analytes and folding energies under the experimental conditions (22^{o}C, 50 mM Tris-HCl, pH 7.4, 50 mM $MgCl_2$). The structures were obtained using Zuker's Mfold software [1].

Comparison of the secondary structure energy of MT1 with other analytes suggests that MT1 forms a less stable secondary structure, which favours the hybridization with the sensors and results in the production of high fluorescence signals. It is important to note that the 3' terminal hairpin of MT6 structure is more stable than in MT1. At the same time, the four 5'-terminal nucleotides AGCG of the hairpin are also a part of the Sensor 1 binding site (see Figure S2A). This secondary structural arrangement may disfavour hybridization of Sensor 1 to the fully complementary MT6 (as well as to all other analytes with exception of MT1) and thus reduce overall fluorescent signal. This may explain the observed lower intensity of Sensor 1 in the presence of complementary MT6 than that in the presence of MT1 (compare bars for MT1 and MT6 in Figure S2B).

3. Design and fluorescent data for Sensor 1.

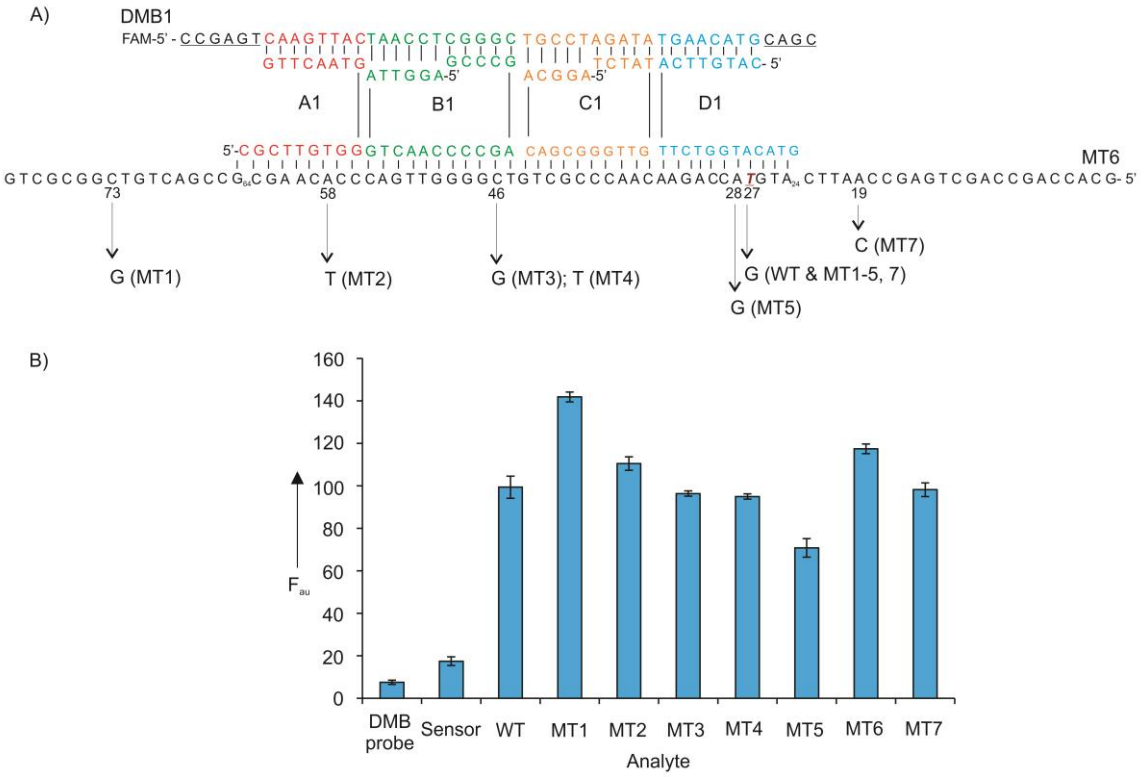

Figure S2. The structure and performance of Sensor 1. A) Schematic diagram of the fluorescent complex of Sensor 1 with MT6 analyte. B) Fluorescent of Sensor 1 in the presence of 8 different analytes (WT and MT1-7). The data are average values of three independent trials with standard deviations.

Sensor 1 was fully complementary to MT6 analyte and had one or two mismatches with other analytes. Four levels of fluorescent intensities can be distinguished for this sensor. The highest fluorescence of the sensor was triggered by MT1 analyte; the second highest fluorescence was produced in the presence of MT2 and MT6, third highest was generated in the presence of WT, MT3 MT4 and MT7, and the lowest fluorescence was triggered by MT5.

Note: The concentration for each adaptor stand was chosen based on the criteria found in Table 1.

4. Design and fluorescent data for Sensor 2.

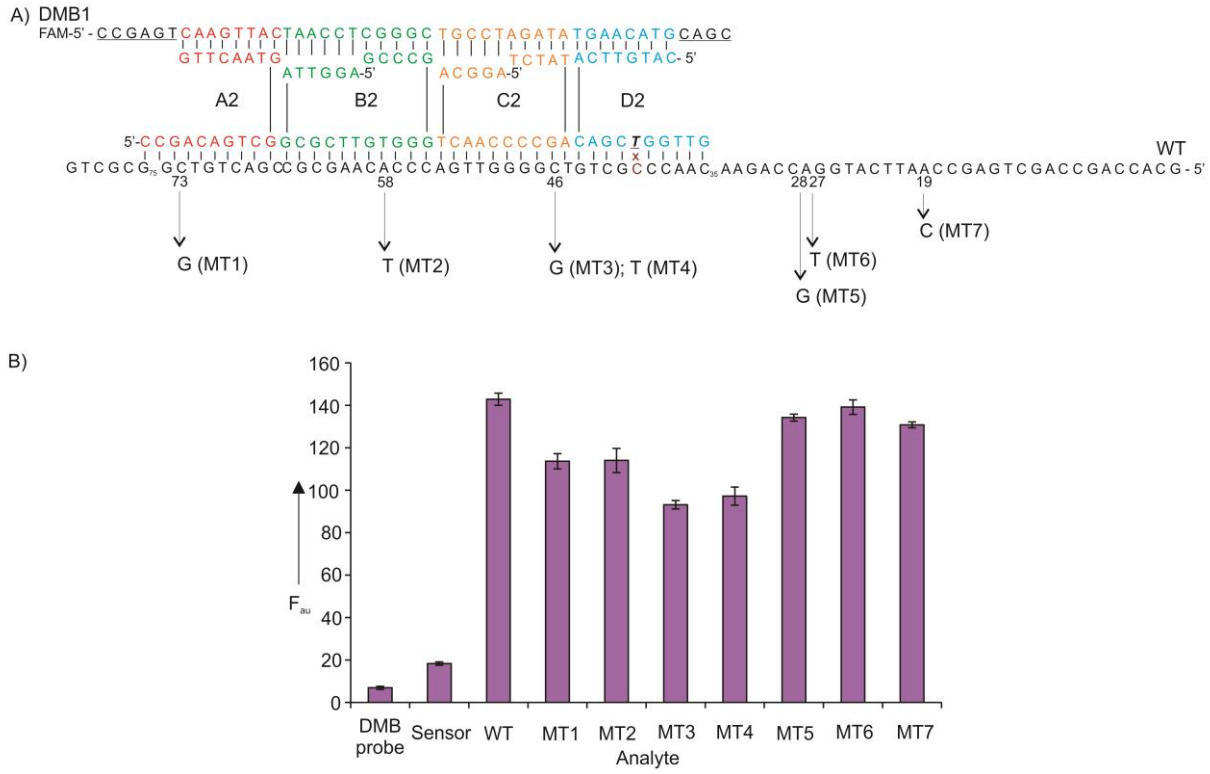

Figure S3. The structure and performance of Sensor 2. A) Schematic diagram of the fluorescent complex of Sensor 1 with WT analyte. B) Fluorescence of Sensor 1 in the presence of different analytes. The data are average values of three independent trials with standard deviations.

Sensor 2 had mismatch with the WT analyte and one or two mismatches with MT1-7 analytes. The introduced mismatches destabilized the complex and improved differentiation of the analytes. The sensor differentiated WT from MT1, MT2, MT3 and MT4. However, MT5, MT6, MT7 triggered the signals of the same intensity as WT. Overall, three levels of the signal were identified; the highest signal was induced by WT, MT5, MT6 and MT7, the intermediate intensity was achieved in the presence of MT1 and MT2, and the lowest fluorescence was observed in the presence of MT3 and MT4.

Note: The concentration for each adaptor stand was chosen based on the criteria described in the footnote to Table 1.

5. Design and fluorescent data for Sensor 3.

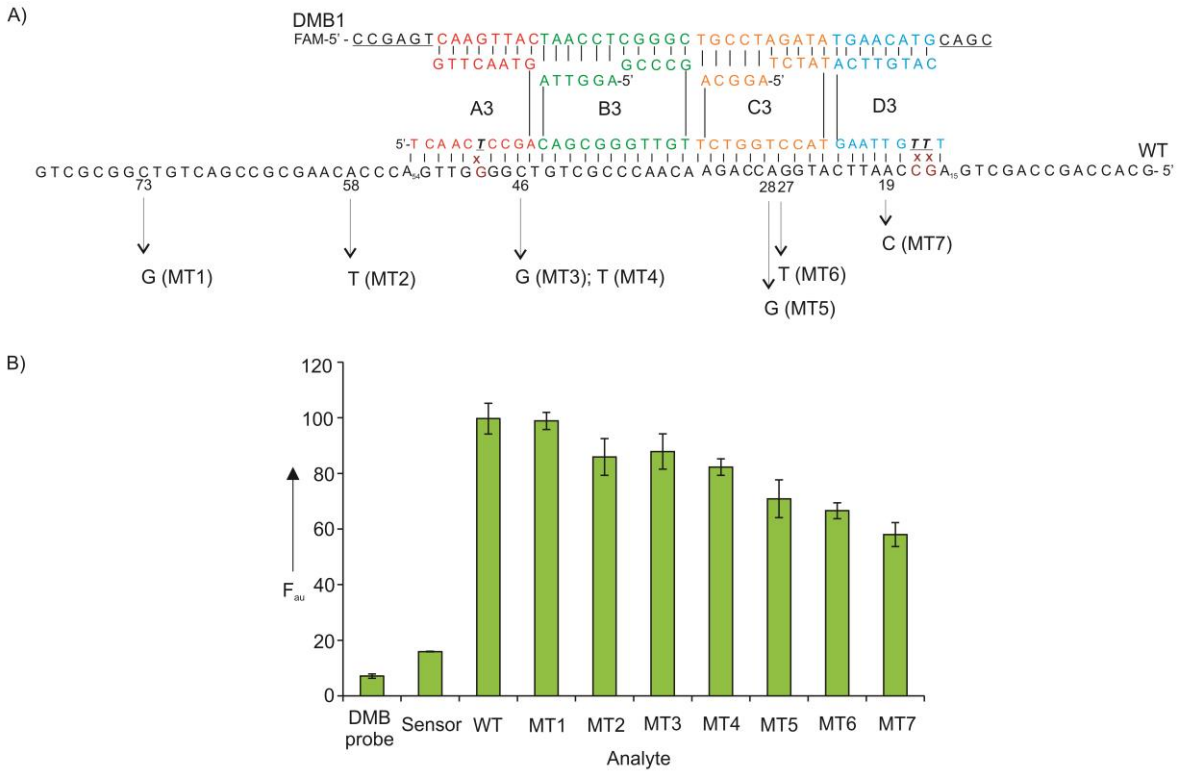

Figure S4. The structure and performance of Sensor 3. A) Schematic diagram of the fluorescent complex of Sensor 3 with WT analyte. B) Fluorescence of Sensor 3 in the presence of different analytes. The data are average values of three independent trials with standard deviations.

Sensor 3 was designed to have three mismatches with WT and three or more mismatches with other analytes. Two mismatches were introduced in the analyte-binding arm of adaptor strand D3 and one mismatch in the strand A3. These mismatches increased the differentiation ability of the sensor: without the mismatches the sensor produced almost equal signal in the presence of each analyte. The first level of differentiation included MT2, which contained a mutation outside of the sensor-recognized region. The absolute fluorescent values for all analytes, however, were lower than that of Sensors 1 and 2; due to the increased instability of the complex. Four levels of signal intensities can be identified; the highest signal was triggered by WT and MT1, second highest by MT2, MT3 and MT4, third highest by MT5 and MT6, and the lowest signal was observed in the presence of MT7.

Note: The concentration for each adaptor stand was chosen based on the criteria described in the footnote to Table 1.

6. Time dependence of fluorescent response of Sensor 1.

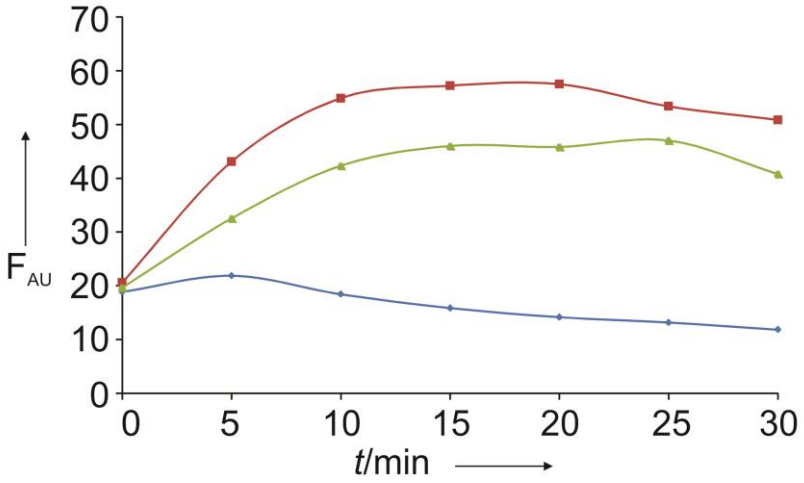

Figure S5. Time dependence of fluorescent response of Sensor 1. The assay was performed as described in Table 1 and the legend of Figure 2. Sensors 1was incubated in the albescence (blue curve) or presence of WT (red), and MT6 (green).

The time dependence of fluorescent responses of the TX sensor to the presence of the analyte revealed that the increase in fluorescent is noticeable right after the addition of the analyte (data not shown) and reaches maximum after 10-15 minute of incubation (Figure S5). The same behaviour was observed for MB-based sensors earlier [2,3].

7. Analysis of MT analytes at different concentrations.

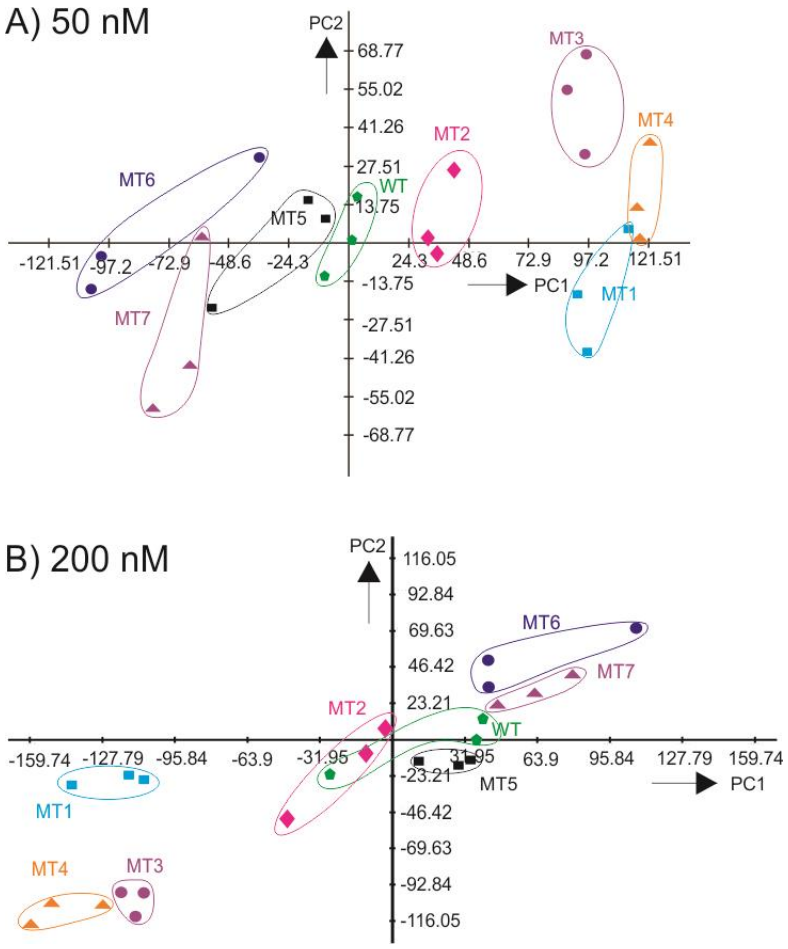

Figure S6. Principal component analysis (PCA) plot of differential fluorescent receptor (DFR) for different concentrations of WT, MT1-MT6 analytes. A) 50 nM and B) 200 nM analytes.

The ability of the differential receptor to distinguish the eight MT analytes at different concentrations was investigated (Figure S6). At 50 nM, the analytes were differentiated with exception of MT1 and MT4, as evident by the non-overlapping clustering of the data (Panel A). For 200 nM analyte the DFR failed in differentiating only WT and MT2 (Panel B). This imperfect behaviour of DFR developed in this proof-of concept study can be fixed by further optimization of the sensors design or by introducing additional TX sensors into the array.

8. References

1. http://mfold.rna.albany.edu/?q=mfold/dna-folding-form.

2. Cornett E.M., O'steen M.R, Kolpashchikov D.M. (2013) Operating cooperatively (OC) sensor for highly specific recognition of nucleic acids. PLOS one 8, e55919.

3. Gerasimova Y.V., Kolpashchikov D.M. (2013) Detection of bacterial 16S rRNA using a molecular beacon-based X sensor. Biosensors & Bioelectronics, 41, 386–390.